Interface focus

J. R. Soc. Interface (2009) **6**, S671–S678
doi:10.1098/rsif.2009.0190.focus
Published online 15 July 2009

Calcium ions induce collapse of charged O-side chains of lipopolysaccharides from *Pseudomonas aeruginosa*

Emanuel Schneck[1], Erzsebet Papp-Szabo[2,3,4], Bonnie E. Quinn[4,5], Oleg V. Konovalov[6], Terry J. Beveridge[2,3,4], David A. Pink[4,5] and Motomu Tanaka[1,4,*]

[1]*Biophysical Chemistry II, Institute of Physical Chemistry and BIOQUANT, University of Heidelberg, 69120 Heidelberg, Germany*
[2]*Department of Molecular and Cellular Biology and* [3]*Biophysics Interdepartmental Group, University of Guelph, Ontario, Canada*
[4]*Advanced Foods and Materials Network of Centres of Excellence, Canada*
[5]*Department of Physics, St Francis Xavier University, Antigonish NS B2G 2W5, Canada*
[6]*European Synchrotron Radiation Facility (ESRF), 38053 Grenoble, Cedex 9, France*

Lipopolysaccharide (LPS) monolayers deposited on planar, hydrophobic substrates were used as a defined model of outer membranes of *Pseudomonas aeruginosa* strain dps 89. To investigate the influence of ions on the (out-of-plane) monolayer structure, we measured specular X-ray reflectivity at high energy (22 keV) to ensure transmission through water. Electron density profiles were reconstructed from the reflectivity curves, and they indicate that the presence of Ca^{2+} ions induces a significant change in the conformation of the charged polysaccharide head groups (O-side chains). Monte Carlo simulations based on a minimal computer model of LPS molecules allow for the modelling of 100 or more molecules over 10^{-3} s and theoretically explained the tendency found by experiments.

Keywords: bacteria; lipopolysaccharide; reflectivity; Monte Carlo simulation

1. INTRODUCTION

Lipopolysaccharides (LPSs) are the main constituents of the outer leaflet of the outer membrane of Gram-negative bacteria (Lüderitz *et al.* 1982). Beyond their structural role, LPSs mediate the interaction of the bacteria with their environment and act as a protection against harmful molecules. Moreover, LPSs function as major virulence factors. The molecules generally consist of a vastly invariant part, constituted by the fundamental building block lipid A and the 'core' oligosaccharide. Lipid A possesses four to seven hydrocarbon chains and two negatively charged glucosamines. In some cases, lipid A contains further substitutions, such as 4-amino-deoxyarabinose, and phosphatidylethanolamine. The core oligosaccharide, typically built from 8–12 sugar units and carrying several negative charges, is connected to the lipid A through a 2-keto-3-deoxyoctonoic acid (2–6 linkage). A variable fraction of LPS molecules possess O-polysaccharides (O-side chains) in the form of repetitive oligosaccharide motives (Caroff & Karibian 2003).

*Author for correspondence (tanaka@uni-heidelberg.de).

One contribution of 13 to a Theme Supplement 'Biological physics at large facilities'.

Pseudomonas aeruginosa is involved in respiratory tract infections and is often associated with chronic infections in cystic fibrosis patients (Høiby 1992). It produces two different types of O-side chains: the A-band polysaccharide is a polymer of uncharged D-rhamnose trisaccharides (Arsenault *et al.* 1991), whereas the B-band is generally built from charged di- to pentasaccharide units. The studied A–B+ LPS lacks the A-band, and its negatively charged B-band polysaccharide is a polymer of trisaccharide repeat units: 2-acetamido-2,6-dideoxy-D-galactose (*N*-acetyl-D-fucosamine), 2,3-diacetamido-2,3-dideoxy-D-mannuronic acid and 3-acetamidino-2-acetamido-2,3-dideoxy-D-mannuronic acid (Knirel *et al.* 1988). Each repeat unit carries two negative charges at environmental pH. The length of the B-band polysaccharide can reach beyond 50 repeat units (Lam *et al.* 1992; Sadovskaya *et al.* 2000) but ranges typically from 20 to 50 repeat units (Daniels *et al.* 2002). However, the major components of LPSs carry either no O-side chain (called 'rough' LPS) or only one repeat unit (called 'semi-rough' LPS). The structure of the studied LPS molecules is presented in figure 1. Since the first report of Brock (1958), several *in vivo* studies have demonstrated that, in the presence of divalent cations

Received 18 May 2009
Accepted 19 June 2009

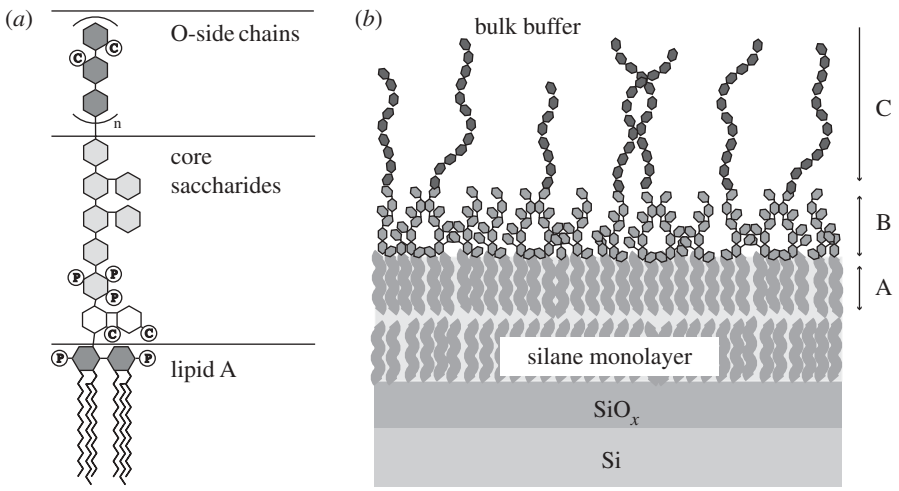

Figure 1. (*a*) Schematic structure of the studied LPS molecules. P, phosphate groups; C, carboxylate groups. (*b*) Solid-supported LPS monolayer under bulk buffer. A, hydrocarbon chain layer; B, dense core saccharide layer; C, sparse O-side chain region.

(Ca^{2+} and Mg^{2+}), bacteria are resistant against cationic antimicrobial peptides such as protamine (pI 10–12) from sperm cells of vertebrates (Islam *et al.* 1984; Hansen *et al.* 2001). The detailed investigation of this phenomenon is of importance for the fundamental understanding of the function of antimicrobial peptides as well as for the development of peptide-based antibiotics (Hancock & Chapple 1999).

There have been several theoretical approaches to model the conformations of LPS molecules in the absence and presence of divalent cations using atomic-scale molecular dynamic simulations (Kotra *et al.* 1999; Lins & Straatsma 2001; Shroll & Straatsma 2002). Although the simulations suggested the condensation of divalent cations mainly in the core region of LPSs, the volume (containing 16 LPS molecules in the outer surface) and the time window (maximum 1 ns) were insufficient to account for conformational changes of the polysaccharide chains. More recently, Pink *et al.* (2003) employed a 'minimum model' that contains 100 *P. aeruginosa* LPS molecules and carried out Monte Carlo (MC) simulations over more than 1 ms. As a crude approximation, the LPS composition was assumed to be 100 per cent *P. aeruginosa* B-band LPSs that possess relatively short O-side chains with 10 trisaccharide units. Although this approach seemed promising to model the conformation of O-side chains of LPSs, systematic comparisons between simulations and experimental studies under biologically relevant conditions are still missing.

To date, LPSs with various structural complexities have been investigated using X-ray diffraction experiments, including crystallography on the molecular structure (Labischinski *et al.* 1985; Kato *et al.* 1990; Kastowsky *et al.* 1993) and small-angle scattering studies on the polymorphisms of the LPS suspensions (Brandenburg & Seydel 1984; Seydel *et al.* 1989; Snyder *et al.* 1999). Katsaras and co-workers measured specular neutron reflectivity from *P. aeruginosa* LPS multilayers on planar substrates at relative humidities up to 85 per cent, corresponding to an osmotic pressure of greater than 10^7 Pa (Abraham *et al.* 2007; Kucerka *et al.* 2008). However, experiments on a single LPS membrane in bulk water (i.e. $\Pi_{H_2O} = 0$) would be more suited for studying the influence of ions in aqueous solutions on the saccharide chain conformation. In our recent account, we measured grazing-incidence X-ray scattering of the monolayer of rough mutant LPS from *Salmonella enterica* sv. *Minnesota* at the air/water interface and demonstrated the Ca^{2+}-induced increase in the electron density near the charged core saccharides (Oliveira *et al.* 2009). However, this strategy could not be easily extended to LPSs with long, polydispersive O-side chains owing to the difficulty in determining the amount of the molecules spread at the air/water interface.

In the present paper, we deposited the monolayer of LPS from *P. aeruginosa* dps 89 (figure 1*a*) onto solid substrates coated with alkylsilane monolayers that mimic the inner leaflet of the outer membrane of bacteria that consists mostly of phosphatidylethanolamine (Rana *et al.* 1991) (figure 1*b*). The LPS monolayers supported by hydrophobic silane monolayers were subjected to specular X-ray reflectivity. Here, a high-energy X-ray beam (22 keV) (Miller *et al.* 2005; Nováková *et al.* 2006) was used in order to ensure the transmission of X-rays through the approximately 20 mm thick water reservoir. The measured signals were modelled using analytically parameterized electron density profiles, which were compared with MC simulations based on a minimal computer model of LPS surfaces. The details of the obtained results are discussed in the following sections.

2. MATERIAL AND METHODS

2.1. Purification and characterization of lipopolysaccharides from PAO1 mutant

Cultures of *P. aeruginosa* dps 89 (A–B+ mutant of the PAO1 strain) (Lightfoot & Lam 1991; Kadurugamuwa *et al.* 1993) were grown to a late logarithmic phase in trypticase soy broth (BBL; 37°C, 125 r.p.m.), and LPS was isolated with the hot phenol–water method

(Westphal & Jann 1965) with several modifications: 3 g of dried cell mass was suspended in 360 ml of water and the temperature was increased to 68°C. Subsequently, a 240 ml portion of liquid phenol was added to the suspension while the temperature was kept at 68°C. The extraction process was carried out for 3 h with constant stirring, and phase separation was allowed to take place in an ice bath overnight. After carefully removing the aqueous phase, another 300 ml portion of water was added to the remaining phenol phase and the extraction step was repeated. The two water fractions were combined and dialysed (molecular weight cut-off (MWCO): 1000 Da) for 3 days against water to remove residual phenol. The extracts were lyophilized, and the dried material was taken up in 80 ml 5 mM Tris/HCl buffer (pH 8.0), containing 1.5 mM $MgCl_2$, 0.5 mM $CaCl_2$, 60 $\mu g\,ml^{-1}$ RNase and 30 $\mu g\,ml^{-1}$ DNase. After an overnight incubation at 37°C (150 r.p.m.), a 15 min phenol extraction step was applied with 20 ml phenol at 37°C to remove the enzymes and residual cell debris. The extraction mixture was centrifuged at 4000g for 10 min at room temperature. The supernatant was dialysed against water and ultracentrifuged at 100 000g for 14 h at 4°C. The LPS pellet was resuspended in water and lyophilized. The samples were characterized with SDS–PAGE, Western immunoblotting (developed with monoclonal antibodies specific to A- and B-bands), ^{1}H NMR spectroscopy and sugar composition analysis (Sawardeker *et al.* 1965). The protein contamination of the material was checked by BCA protein assay (Pierce, Rockford, IL, USA) and Lowry total protein assay (Peterson's modification, Sigma-Aldrich, St Louis, MO, USA) and found to be below 1% w/w. There was no detectable DNA and RNA contamination in the LPS sample.

2.2. Chemicals and sample preparation

Unless stated otherwise, all chemicals were purchased from Fluka (Taufkirchen, Germany) and used without further purification. Throughout the study, we used double deionized water with a specific resistance of greater than 18 MΩ cm (MilliQ, Molsheim, France). A rectangular (25 mm × 20 mm) Si(100) substrate with native oxide (Si-Mat, Landsberg/Lech, Germany) was cleaned by a commonly used cleaning process in semiconductor technology (called the RCA method) with a slight modification (Kern & Puotinen 1970). A self-assembled monolayer of octadecyltrimethoxysilane (ODTMS, purchased from ABCR, Karlsruhe, Germany) was covalently grafted onto the substrate according to Hillebrandt & Tanaka (2001). Subsequently, the substrate was stored at 70°C for 3 h and in a vacuum chamber overnight to remove residual solvent molecules. Finally, the functionalized substrate was inserted into a self-built liquid cell. LPS was suspended in 5 mM HEPES and 100 mM KCl at pH 7.4 (called 'Ca^{2+}-free buffer' in the following) at a concentration of 5 $mg\,ml^{-1}$. After sonication with a tip sonifier (Misonix, Newtown, CT, USA) under mild conditions (interval mode: 0.5 s/0.5 s on/off, constant cooling to $T < 50$°C), the LPS suspension was diluted with Ca^{2+}-free buffer to a final concentration of 1 $mg\,ml^{-1}$. The LPS suspension was injected into the liquid cell and incubated at 50°C for 1 h. After extensive rinsing, the sample was subjected to the reflectivity measurement in Ca^{2+}-free buffer. In the next step, the liquid cell was rinsed with an excess of 'Ca^{2+}-loaded buffer' (5 mM HEPES, 100 mM KCl and 50 mM $CaCl_2$, pH 7.4) for the reflectivity measurements in the presence of Ca^{2+} ions.

2.3. Specular X-ray reflectivity

Specular X-ray reflectivity experiments were carried out at the ID10B beamline at ESRF (Grenoble, France). The monochromatic beam with a photon energy of 22 keV was collimated to a vertical beam aperture of 20 μm. At each angle of incidence α_i, corresponding to the momentum transfer perpendicular to the interface $q_z = 4\pi/\lambda \sin \alpha_i$, the reflectivity was corrected for the beam footprint and for the beam intensity (via an in-beam monitor). To highlight the changes in the measured intensities, the reflectivity curves were multiplied by q_z^4 for all presentations. The electronic structure of the solid-supported LPS monolayer was represented by an analytical profile function (see §3 for details), characterized by a set of free fitting parameters. The analytical electron density profile was split into a set of 1 Å thick slabs with different electron densities. These slabs were treated using the Parratt formalism (Abelès 1950; Parratt 1954) to compute the corresponding specular reflectivity curve as a function of q_z. According to the high resolution (1 Å) of the slab profiles, it was not necessary to include slab roughnesses in these calculations (Nevot & Croce 1980). The free parameters were varied to achieve the minimum in the χ^2 deviation between experimental results and simulations.

2.4. Monte Carlo simulations

To simulate the saccharide conformation of the LPS monolayer in the absence and presence of Ca^{2+}, we employed a 'minimal computer model' (Pink *et al.* 2003) using linearized Poisson–Boltzmann theory (Israelachvili 1985; Deserno *et al.* 2000) and carried out MC simulations employing the Metropolis algorithm (Binder 1988; Lai & Binder 1992). The aqueous region of the simulation volume ranged from $z = 0$ to $z = 300$ Å. To take thermal fluctuations of saccharide chains into account, we set the resolution of our theoretical slabs to be approximately 2 Å. However, it should be noted that our simulations with 100 LPS molecules cannot take the statistical roughness of the interface into account. The level of $z = 0$ was defined as the boundary between the aqueous solution ($z > 0$) and the hydrocarbon chain region ($z < 0$), which were represented as two dielectric continua with relative permittivities $\varepsilon_w = 81$ and $\varepsilon_{hc} = 5$, respectively (Israelachvili 1985; Pink *et al.* 1997). We represented monovalent ion screening in the aqueous solution by the linearized Poisson–Boltzmann theory (Israelachvili 1985; Vlachy 1999; Deserno *et al.* 2000; Pink *et al.* 2003) and calculated electrostatic interactions according to the expression derived by Netz (1999). A more detailed description is given elsewhere (Pink *et al.* 2003; Oliveira

et al. 2009). In the model, each saccharide group of an LPS molecule was represented by a sphere of radius $r_{\mathrm{sugar}} = 1.5$ Å, connected by stretchable bonds with equilibrium lengths L_0 (Carmesin & Kremer 1988; Chakrabarti et al. 1994). We restricted the relative angle between the saccharide–saccharide bonds of these semi-flexible molecules to be $30 \pm 10^{\circ}$ (Pink et al. 2003). Negatively charged sugars possessed charge −1 in units of $e = 1.6 \times 10^{-19}$ C at their centres. To account for attractive short-range interactions between saccharides, a pair of sugar spheres was allowed to form a bond with the binding energy $E_{\mathrm{B}} = 0.4 \times 10^{-20}$ J, when they are closer than the critical distance of $R_{\mathrm{B}} = 2.0$ Å. This binding energy is comparable to a typical value for hydrogen bonds and van der Waal interactions. The hydrocarbon chain moieties of a molecule were represented by two spheres, each of which had a radius of $R_{\mathrm{A}} = 7.0$ Å. The one connected to the core saccharides possessed an equilibrium position at $z = -4.0$ Å and could move along the z-axis by $\Delta z = \pm 1.5$ Å. The second sphere was connected to the first sphere via a centre-to-centre bond that could stretch from 10 to 15 Å. Anchoring spheres were allowed to rotate around their centre, but no saccharide group or ion was allowed to move into the region $z < 0$. Hydrated ions were represented by spheres of radius $R_{\mathrm{I}} = 1.8$ Å, whose charges were located at their centres. We used an implicit monovalent ionic strength of 25 mM (corresponding to $\kappa^{-1} \cong 20$ Å) and added sufficient explicit monovalent ions to match the bulk concentration used in the experiments. The 'bulk' was specified to be the upper third of the simulation volume, $200 < z < 300$ Å. The resulting effective screening length was approximately $\kappa^{-1} \cong 10$ Å. In the 'Ca^{2+}-loaded' case, the system additionally contained a number of Ca^{2+} ions and twice as many Cl^{-} ions, such that the desired concentration was reached in the bulk. The system was equilibrated to $T = 300$ K for 2×10^6 MC steps, and the properties of the system were measured for a further 0.5×10^6 steps.

3. RESULTS AND DISCUSSION

3.1. Characterization of lipopolysaccharides

Figure 2 shows the Western immunoblotting developed with monoclonal antibodies specific to A-band (figure 2*a*) and B-band (figure 2*b*), which proves the lack of A-band polysaccharides in the A–B+. In fact, the B-band pattern of A–B+ LPS is very similar to that of the PAO1 strain. Moreover, the SDS–PAGE pattern of A–B+ LPS was very similar to that of PAO1 LPS (E. Papp-Szabo 2008, unpublished data). These results suggest that the composition of the studied A–B+ LPS should be comparable to that of PAO1 LPS (70% rough, 20% semi-rough and 10% LPS with B-band polysaccharides), determined by size exclusion chromatography, NMR spectroscopy and sugar-composition analysis (unpublished data). Considering the similarities in the B-band patterns between these two strains, the B-band polysaccharides in the studied A–B+ LPS should have a length distribution similar to those in PAO1 LPS: 20–50 repeat units (Daniels et al. 2002).

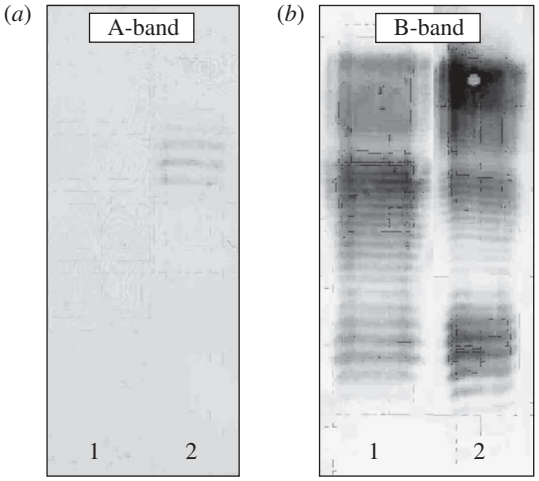

Figure 2. Western immunoblotting patterns of LPS molecules developed with monoclonal antibodies specific to A-band (*a*) and B-band (*b*). 1, A–B+ LPS; 2, PAO1 LPS.

3.2. Specular X-ray reflectivity

Figure 3*a* shows the reflectivity curves $R \times q_z^4$ measured in Ca^{2+}-free buffer and Ca^{2+}-loaded buffer, showing a clear difference in the global shape of the reflectivity curves. The measured reflectivity signals from the stratified system (figure 1*b*) were analysed with the following simplified model. First, the Si substrate was treated as a semi-infinite medium with a constant electron density ρ_{Si}. For simplicity, the native silicon oxide layer that has almost identical electron density was considered as part of the Si medium. The hydrocarbon chain region, composed of the substrate-bound ODTMS layer and the LPS hydrocarbon chain layer, was considered as one single slab with constant electron density ρ_{HC} and thickness d_{HC}. The saccharide head groups were represented by two sections: one slab with constant electron density ρ_{S} and thickness d_{S} and the other section in which the electron density continuously decays towards that of the bulk buffer ρ_{B}. The former corresponds to the compact invariant part of the core saccharides, whereas the latter represents sparse and polydisperse O-side chains (figure 1*a*). We accounted for roughnesses at the Si/hydrocarbon and hydrocarbon/core saccharide interfaces by modelling the electron density gradients as error functions, characterized by the r.m.s. roughness $\sigma_{\mathrm{Si}\rightarrow\mathrm{HC}}$ and $\sigma_{\mathrm{HC}\rightarrow\mathrm{S}}$, respectively. This approach is commonly taken to describe the roughness in slab models in X-ray and neutron reflectivity studies (Tidswell et al. 1990; Doshi et al. 2005; Rehfeldt et al. 2006; Schubert et al. 2008). However, since polydispersive O-side chains are grafted at a low surface density (approx. 10%), it is not realistic to use the slab model to describe the density profile of the O-side chains in buffer. We account for the continuous decay of the electron density towards bulk buffer using a stretched exponential decay function, characterized by the decay length Λ and the stretching exponent h. Throughout the data analysis, the values for ρ_{Si} and ρ_{B} were taken from the literature. Furthermore, we fitted the thickness and electron density of the hydrocarbon region (ρ_{HC} and d_{HC},

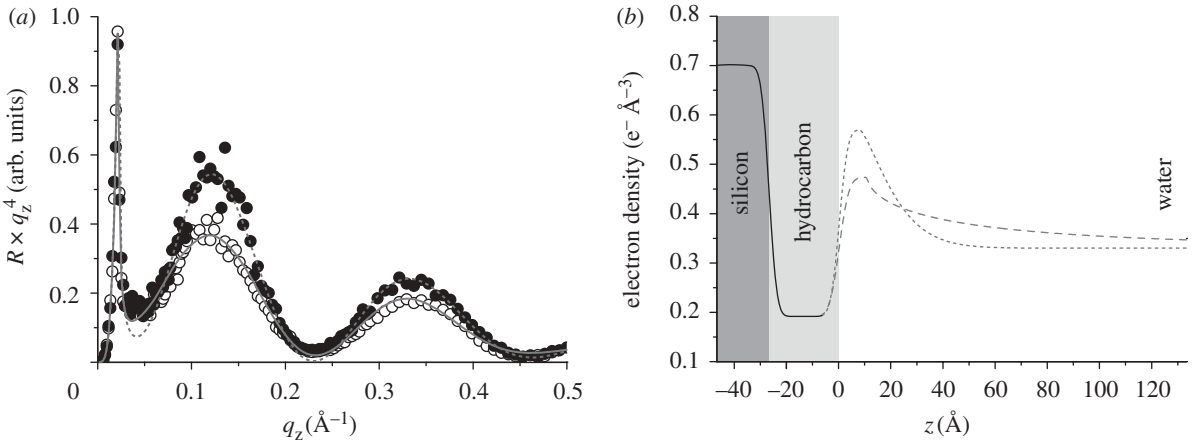

Figure 3. (*a*) Reflectivity curves of solid-supported LPS monolayer in Ca^{2+}-free (open circles) and Ca^{2+}-loaded (filled circles) buffers. Solid and dashed lines represent the fits corresponding to the best-matching model parameters. (*b*) Electron density profiles corresponding to the best-matching model parameters. The interface between hydrocarbon slab and core saccharide slab coincides with $z = 0$. The core saccharides and O-side chains exhibit a significant difference in the conformation in the absence (dashed line) and presence (dotted line) of Ca^{2+}. Solid line, common model.

respectively) and the roughness of the Si/hydrocarbon interface $\sigma_{Si\rightarrow HC}$ simultaneously in the presence and absence of Ca^{2+} to achieve a common parameter set for $z < 0$. This simplification would be justified as the reflectivity measurements were successively carried out with the same sample in Ca^{2+}-free and Ca^{2+}-loaded buffers.

In figure 3*a*, the best-fit results in Ca^{2+}-free and Ca^{2+}-loaded buffers are superimposed to the corresponding reflectivity curves, and the model parameters used for the analysis are summarized in table 1.[1] The electron density profiles reconstructed from the models are shown in figure 3*b*. Although the five free fitting parameters imply a certain ambiguity of the model, the presented model seems more realistic than others with a comparably low χ^2. For example, in contrast to other models, the presented one fulfils the requirement of the electron number conservation near the interface, which is reflected by the integrated electron density profiles (figure 3*b*).

The electron density of the 'unified' hydrocarbon slab (chains from LPS and silane), $\rho_{HC} = 0.19\ e^-\ Å^{-3}$, is smaller than the value we reported previously for rough mutant LPS monolayers ($\rho \cong 0.3\ e^-\ Å^{-3}$) at the air/water interface (Oliveira *et al.* 2009). This can be attributed either to the lower lateral density of chains in ODTMS and LPS monolayers or to the local density minimum between two opposing hydrocarbon chains (called 'methyl dip'), which was not explicitly included in our model in order to minimize the number of parameters.

The reconstructed electron density profiles (figure 3*b*) indicate that the presence of Ca^{2+} ions induces two prominent differences. First, the electron density in the core saccharide slab in the presence of Ca^{2+} ($\rho_S = 0.57\ e^-\ Å^{-3}$) is significantly higher (approx. 20%) than the corresponding value in Ca^{2+}-free buffer ($\rho_S = 0.47\ e^-\ Å^{-3}$). Second, in Ca^{2+}-loaded buffer, the electron density of the O-side chain region decays much steeper to the level of the bulk buffer at $z > 10$ Å, which coincides with a significant increase in the stretching exponent (from $h_{Ca^{2+}\text{-free}} = 0.30$ to $h_{Ca^{2+}\text{-loaded}} = 0.68$) and a decrease in the decay length (from $\Lambda_{Ca^{2+}\text{-free}} = 34.4$ Å to $\Lambda_{Ca^{2+}\text{-loaded}} = 15.6$ Å).

Table 1. Best-fit parameters used to represent the reflectivity curves in Ca^{2+}-free and Ca^{2+}-loaded buffer.

common parameters		
$\sigma_{Si\rightarrow HC}$ (Å)	2.3	
ρ_{HC} (e$^-$ Å^{-3})	0.19	
d_{HC} (Å)	26.9	
free parameters	*Ca^{2+}-free*	*Ca^{2+}-loaded*
$\sigma_{HC\rightarrow S}$ (Å)	2.9	2.6
ρ_S (e$^-$ Å^{-3})	0.47	0.57
d_S (Å)	10.7	7.8
Λ (Å)	34.4	15.6
h	0.30	0.68

3.3. Monte Carlo simulations

MC simulations were carried out to simulate the conformation of LPS molecules in the absence and presence of divalent cations, mimicking the experimental conditions in Ca^{2+}-free and Ca^{2+}-loaded buffers. In our computer model, we assumed that 10 per cent of the LPS molecules possess an O-side chain, whereas 90 per cent of the molecules (including 70% rough and 20% semi-rough LPSs) are all rough LPSs.[2]

[1]In this study, a high Ca^{2+} concentration (50 mM) was used for the direct comparison with the MC simulation results. In fact, our preliminary experiments suggested that 5 mM Ca^{2+} seems sufficient to induce the observed conformational changes. Further details on the influence of [Ca^{2+}] are currently under investigation.

[2]The presented model considers more realistic conditions than the previous account (Pink *et al.* 2003), which assumed that all the LPS molecules possess O-side chains with 10 repeat units. On the other hand, the conformational change in the O-side chains discussed in this paper seems to be a cooperative process, as a longer single O-side chain (with 40 repeat units) showed no collapse in the presence of Ca^{2+} ions (data not shown).

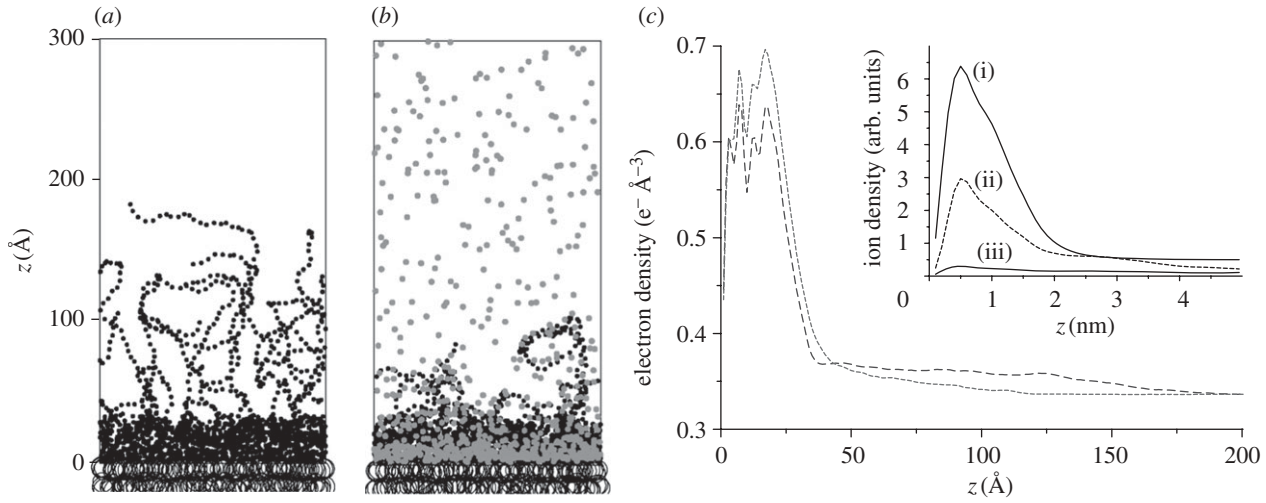

Figure 4. Instantaneous pictures of the computer simulation after equilibration in the absence (*a*) and presence (*b*) of Ca^{2+}. Hydrocarbon moieties are indicated by open large circles, saccharide groups by small filled black circles and Ca^{2+} ions by small filled grey circles. Monovalent ions (K^+ and Cl^-) are not shown. (*c*) Time-averaged electron density profiles in the aqueous region ($z > 0$) calculated from the computer simulations in the absence (broken line) and presence (dashed line) of Ca^{2+}. The inset shows the time-averaged number distributions of: (i) K^+ in the absence of Ca^{2+}, (ii) Ca^{2+} and (iii) K^+ in the presence of Ca^{2+}.

The characteristic length and time scales of the simulations had to be sufficient to model a system with ionic concentrations giving rise to a Debye screening length of $\kappa^{-1} \cong 10$ Å. We used periodic boundary conditions (PBCs) in directions parallel to the surface of the monolayer, but not perpendicular to it. Accordingly, we had to ensure that O-side chains anchored in the monolayer have no correlation with themselves via PBCs and that the bulk region is sufficiently far from the monolayer. We set the length of the O-side chains to be 20 repeat units (60 saccharides) in order to minimize the simulation volume, which seems reasonable to describe natural B-band polysaccharides with 20–50 repeating units. Accordingly, the average membrane plane (*xy*-plane) of our simulation volume possessed 100 LPS molecules, of which 10 randomly chosen ones (10%) possessed O-side chains.

Figure 4*a*,*b* presents instantaneous pictures of the simulation volume after equilibration in Ca^{2+}-free and Ca^{2+}-loaded buffers, respectively. The pictures show a significant change in the conformation of LPS molecules: the long O-side chains collapse towards the core saccharide region in the presence of Ca^{2+}. This effect was quantified by calculating the time-averaged vertical electron density profiles in the aqueous region ($z > 0$) from the computer simulations (figure 4*c*). The profiles show that Ca^{2+} induces a clear increase in the electron density in the core saccharide region, while the tail of the distribution decays to the bulk buffer level $\rho_B = 0.33\ e^-\ Å^{-3}$ at much lower z in Ca^{2+}-loaded buffer. Furthermore, the time-averaged number density profiles of cations (figure 4*c*, inset) predict that Ca^{2+} ions condense in the negatively charged core saccharide region and almost completely displace monovalent K^+ ions from this region. It should be noted that we found no clear sign of aggregation of the O-side chains in the absence of Ca^{2+}, despite significant electrostatic screening ($\kappa^{-1} \cong 1$ nm). This indicates that the strong electrostatic repulsion between negatively charged saccharide chains prohibits the aggregation, although we allow for attractive short-range interactions between saccharides in our simulation. In contrast, in the presence of Ca^{2+}, O-side chains are bound together via dynamic Ca^{2+} bridging (figure 4*b*), which is enhanced by the attractive short-range interactions between saccharide moieties. As a result, the O-side chains undergo a massive collapse towards the surface of dense core saccharides.

The electron density profiles from the computer simulations in the absence and presence of Ca^{2+} can be directly compared with the experimental results. The calculated profiles show the same tendency as those reconstructed from the measured reflectivity curves (figure 3*b*): Ca^{2+} induces a significant electron density increase in the core saccharide region, and the electron density decays steeply to the bulk level in the presence of Ca^{2+}. Last but not the least, differences in absolute electron density values and the detailed shape of the electron density profiles between experiments and computer simulations can be attributed to the uncertainty (approx. 15%) in the lateral density of the LPS monolayer as well as to the lack of semi-rough LPSs in the computer simulation.

4. CONCLUSIONS

We created a well-defined model of the outer membranes of bacteria by the deposition of a monolayer of purified LPSs onto a planar substrate functionalized with an alkyl silane monolayer. This system is ideally suited for the characterization of the out-of-plane membrane structure in bulk buffer solution using high-energy specular X-ray reflectivity. In this study, we investigated the influence of divalent cations on the conformation of the charged O-side chains of LPS from *P. aeruginosa* dps 89. The electron density profiles

of the monolayer, reconstructed from the reflectivity measurements in the absence and presence of Ca^{2+}, indicated that the O-side chains collapse towards the LPS core saccharide region in the presence of Ca^{2+} ions. To simulate the ion-induced conformational change of LPS molecules implied by the experimental results, we created a minimal computer model system that contains 10 per cent of the LPS molecules with O-side chains. Monte Carlo simulations based on the minimal model consistently indicated the same tendency as the experimental finding. The obtained results reveal that the condensation of divalent ions (Ca^{2+}) in the negatively charged core saccharides and the collapse of O-side chains are the principal mechanisms of the resistance of bacteria to cationic antimicrobial peptides. Thus, the combination of high-energy specular X-ray reflectivity and Monte Carlo simulation is a powerful technique for the detailed structural characterization of complex biological interfaces buried under aqueous media.

M.T. thanks the German Science Foundation for support (Ta 259/6). E.S. thanks the State Baden-Württemberg and DAAD for fellowships. D.A.P. is thankful to the Natural Sciences and Engineering Research Council of Canada. We thank ESRF for synchrotron beam times, HPClab (St.F.X.U.) and ACENET for computing assistance and the Advanced Foods and Materials Network of Centres of Excellence (AFMNet-NCE) and the Atlantic Innovation Fund for support.

REFERENCES

Abelès, F. 1950 La théorie générale des couches minces. *J. Phys. Radium* **11**, 307–309. (doi:10.1051/jphysrad:01950001107030700)

Abraham, T., Schooling, S. R., Nieh, M., Kucerka, N., Beveridge, T. J. & Katsaras, J. 2007 Neutron diffraction study of *Pseudomonas aeruginosa* lipopolysaccharide bilayers. *J. Phys. Chem. B* **111**, 2477–2483. (doi:10.1021/jp066012+)

Arsenault, T. L., Hughes, D. W., MacLean, D. B., Szarek, W. A., Kropinski, A. M. B. & Lam, J. S. 1991 Structural studies on the polysaccharide portion of 'A-band' lipopolysaccharide from a mutant (AK1401) of *Pseudomonas aeruginosa* strain PAO1. *Can. J. Chem.* **69**, 1273–1280. (doi:10.1139/v91-190)

Binder, K. 1988 *Monte Carlo simulation in statistical physics: an introduction*. Berlin, Germany: Springer.

Brandenburg, K. & Seydel, U. 1984 Physical aspects of structure and function of membranes made from lipopolysaccharides and free lipid A. *Biochim. Biophys. Acta* **775**, 225–238. (doi:10.1016/0005-2736(84)90174-3)

Brock, T. D. 1958 The effect of salmine on bacteria. *Can. J. Microbiol.* **4**, 65.

Carmesin, I. & Kremer, K. 1988 The bond fluctuation method: a new effective algorithm for the dynamics of polymers in all spatial dimensions. *Macromolecules* **21**, 2819–2823. (doi:10.1021/ma00187a030)

Caroff, M. & Karibian, D. 2003 Structure of bacterial lipopolysaccharides. *Carbohydr. Res.* **338**, 2431–2447. (doi:10.1016/j.carres.2003.07.010)

Chakrabarti, A., Nelson, P. & Toral, R. 1994 Interpenetrations in polymer brushes. *J. Chem. Phys.* **100**, 748. (doi:10.1063/1.466945)

Daniels, C., Griffiths, C., Cowles, B. & Lam, J. S. 2002 *Pseudomonas aeruginosa* O-antigen chain length is determined before ligation to lipid A core. *Environ. Microbiol.* **4**, 883–897. (doi:10.1046/j.1462-2920.2002.00288.x)

Deserno, M., Holm, C. & May, S. 2000 Fraction of condensed counterions around a charged rod: comparison of Poisson–Boltzmann theory and computer simulations. *Macromolecules* **33**, 199–206. (doi:10.1021/ma990897o)

Doshi, D. A., Watkins, E. B., Israelachvili, J. N. & Majewski, J. 2005 Reduced water density at hydrophobic surfaces: effect of dissolved gases. *Proc. Natl Acad. Sci. USA* **102**, 9458–9462. (doi:10.1073/pnas.0504034102)

Hancock, R. E. W. & Chapple, D. S. 1999 Peptide antibiotics. *Antimicrob. Agents Chemother.* **42**, 1317.

Hansen, L. T., Austin, J. W. & Gill, T. A. 2001 Antibacterial effect of protamine in combination with EDTA and refrigeration. *Int. J. Food Microbiol.* **66**, 149–161. (doi:10.1016/S0168-1605(01)00428-7)

Hillebrandt, H. & Tanaka, M. 2001 Electrochemical characterization of self-assembled alkylsiloxane monolayers on indium–tin oxide (ITO) semiconductor electrodes. *J. Phys. Chem. B* **105**, 4270–4276. (doi:10.1021/jp004062n)

Høiby, N. 1992 Prevention and treatment of infections in cystic fibrosis. *Int. J. Antimicrob. Agents* **1**, 229–237. (doi:10.1016/0924-8579(92)90033-N)

Islam, N. M., Itakura, T. & Motohiro, T. 1984 Antibacterial characteristics of fish protamines. 1. Antibacterial spectra and minimum inhibition concentration of clupeine and salmine. *Bull. Jpn. Soc. Sci. Fish.* **50**, 1705.

Israelachvili, J. N. 1985 *Intermolecular and surface forces*. London, UK: Academic Press Inc.

Kadurugamuwa, J. L., Lam, J. S. & Beveridge, T. J. 1993 Interaction of gentamicin with the A band and B band lipopolysaccharides of Pseudomonas aeruginosa and its possible lethal effect. *Antimicrob. Agents Chemother.* **37**, 715–721.

Kastowsky, M., Gutberlet, T. & Bradaczek, H. 1993 Comparison of X-ray powder-diffraction data of various bacterial lipopolysaccharide structures with theoretical model conformations. *Eur. J. Biochem.* **217**, 771–779. (doi:10.1111/j.1432-1033.1993.tb18305.x)

Kato, N., Ohta, M., Kido, N., Ito, H., Naito, S., Hasegawa, T., Watabe, T. & Sasaki, K. 1990 Crystallization of R-form lipopolysaccharides from *Salmonella minnesota* and *Escherichia coli*. *J. Bacteriol.* **172**, 1516.

Kern, W. & Puotinen, D. A. 1970 Cleaning solutions based on hydrogen peroxide for use in silicon semiconductor technology. *RCA Rev.* **31**, 187.

Knirel, Y. A., Vinogradov, E. V., Kocharova, N. A., Paramonov, N. A., Kochetkov, N. K., Dmitriev, B. A., Stanislavsky, E. S. & Lányi, B. 1988 O-specific polysaccharides and serological classification of Pseudomoms aeruginosa. *Acta Microbiol. Hung.* **35**, 3.

Kotra, L. P., Golemi, D., Amro, N. A., Liu, G. Y. & Mobashery, S. 1999 Dynamics of the lipopolysaccharide assembly on the surface of *Escherichia coli*. *J. Am. Chem. Soc.* **121**, 8707–8711. (doi:10.1021/ja991374z)

Kucerka, N., Papp-Szabo, E., Nieh, M., Harroun, T. A., Schooling, S. R., Pencer, J., Nicholson, E. A., Beveridge, T. J. & Katsaras, J. 2008 Effect of cations on the structure of bilayers formed by lipopolysaccharides isolated from *Pseudomonas aeruginosa* PAO1. *J. Phys. Chem. B* **112**, 8057–8062. (doi:10.1021/jp8027963)

Labischinski, H., Barnickel, G., Bradaczek, H., Naumann, D., Rietschel, E. T. & Giesbrecht, P. 1985 High state of order of isolated bacterial lipopolysaccharide and its possible contribution to the permeation barrier property of the outer membrane. *J. Bacteriol.* **162**, 9.

Lai, P. Y. & Binder, K. 1992 Structure and dynamics of polymer brushes near the **Θ** point: a Monte Carlo simulation. *J. Chem. Phys.* **97**, 586. (doi:10.1063/1.463554)

Lam, J. S., Graham, L. L., Lightfoot, J., Dasgupta, T. & Beveridge, T. J. 1992 Ultrastructural examination of the lipopolysaccharides of Pseudomonas aeruginosa strains and their isogenic rough mutants by freeze-substitution. *J. Bacteriol.* **174**, 7159.

Lightfoot, J. & Lam, J. S. 1991 Molecular cloning of genes involved with expression of A-band lipopolysaccharide, an antigenically conserved form, in Pseudomonas aeruginosa. *J. Bacteriol.* **173**, 5624.

Lins, R. D. & Straatsma, T. P. 2001 Computer simulation of the rough lipopolysaccharide membrane of *Pseudomonas aeruginosa*. *Biophys. J.* **81**, 1037–1046. (doi:10.1016/S0006-3495(01)75761-X)

Lüderitz, O., Freudenberg, M., Galanos, C., Lehmann, V., Rietschel, E. T. & Shaw, D. H. 1982 Lipopolysaccharides of gram-negative bacteria. *Curr. Top. Membr. Transp.* **17**, 79.

Miller, C. E., Majewski, J., Gog, T. & Kuhl, T. L. 2005 Characterization of biological thin films at the solid–liquid interface by X-ray reflectivity. *Phys. Rev. Lett.* **94**, 238104. (doi:10.1103/PhysRevLett.94.238104)

Netz, R. R. 1999 Debye–Hückel theory for interfacial geometries. *Phys. Rev. E* **60**, 3174–3182. (doi:10.1103/PhysRevE.60.3174)

Nevot, L. & Croce, P. 1980 Caractérisation des surfaces par réflexion rasante de rayons X. Application à l'étude du polissage de quelques verres silicates. *Rev. Phys. Appl.* **15**, 761–779. (doi:10.1051/rphysap:01980001503076100)

Nováková, E., Giewekemeyer, K. & Salditt, T. 2006 Structure of two-component lipid membranes on solid support: an x-ray reflectivity study. *Phys. Rev. E* **74**, 05.

Oliveira, R. G. *et al.* 2009 Physical mechanisms of bacterial survival revealed by combined grazing-incidence X-ray scattering and Monte Carlo simulation. *C. R. Chimie* **12**, 209–217. (doi:10.1016/j.crci.2008.06.020)

Parratt, L. G. 1954 Surface studies of solids by total reflection of X-rays. *Phys. Rev.* **95**, 359–369. (doi:10.1103/PhysRev.95.359)

Pink, D. A., Belaya, M., Levadny, V. & Quinn, B. 1997 A model of polar group statics in lipid bilayers and monolayers. *Langmuir* **13**, 1701–1711. (doi:10.1021/la950343o)

Pink, D. A., Hansen, L. T., Gill, T. A., Quinn, B. E., Jericho, M. H. & Beveridge, T. J. 2003 Divalent calcium ions inhibit the penetration of protamine through the polysaccharide brush of the outer membrane of Gram-negative bacteria. *Langmuir* **19**, 8852–8858. (doi:10.1021/la030193e)

Rana, F. R., Sultany, C. M. & Blazyk, J. 1991 Determination of the lipid composition of *Salmonella typhimurium* outer membranes by ^{31}P NMR. *J. Microbiol. Methods* **14**, 41–51. (doi:10.1016/0167-7012(91)90006-C)

Rehfeldt, F., Steitz, R., Klitzing, R. v., Armes, S. P., Gast, A. P. & Tanaka, M. 2006 Reversible activation of diblock copolymer monolayers at the interface by pH modulation, 1: lateral chain density and conformation. *J. Phys. Chem. B* **110**, 9171–9176. (doi:10.1021/jp054532j)

Sadovskaya, I., Brisson, J. R., Thibault, P., Richards, J. C., Lam, J. S. & Altman, E. 2000 Structural characterization of the outer core and the O-chain linkage region of lipopolysaccharide from *Pseudomonas aeruginosa* serotype O5. *Eur. J. Biochem.* **267**, 1640–1650. (doi:10.1046/j.1432-1327.2000.01156.x)

Sawardeker, J. S., Sloneker, J. H. & Jeanes, A. 1965 Quantitative determination of monosaccharides as their alditol acetates by gas liquid chromatography. *Anal. Chem.* **37**, 1602–1604. (doi:10.1021/ac60231a048)

Schubert, T., Seitz, P., Schneck, E., Nakamura, M., Shibakami, M., Funari, S. S., Konovalov, O. & Tanaka, M. 2008 Structure of synthetic transmembrane lipid membranes at the solid/liquid interface studied by specular X-ray reflectivity. *J. Phys. Chem. B* **112**, 10 041–10 044. (doi:10.1021/jp803937m)

Seydel, U., Brandenburg, K., Koch, M. H. J. & Rietschel, E. T. 1989 Supramolecular structure of lipopolysaccharide and free lipid A under physiological conditions as determined by synchrotron small-angle X-ray diffraction. *Eur. J. Biochem.* **186**, 325–332. (doi:10.1111/j.1432-1033.1989.tb15212.x)

Shroll, R. M. & Straatsma, T. P. 2002 Molecular structure of the outer bacterial membrane of *Pseudomonas aeruginosa* via classical simulation. *Biopolymers* **65**, 395–407. (doi:10.1002/bip.10279)

Snyder, S., Kim, D. & McIntosh, T. J. 1999 Lipopolysaccharide bilayer structure: effect of chemotype, core mutations, divalent cations, and temperature. *Biochemistry* **38**, 10 758–10 767. (doi:10.1021/bi990867d)

Tidswell, I. M., Ocko, B., Pershan, P. S., Wasserman, S. R., Whitesides, G. M. & Axe, J. D. 1990 X-ray specular reflection studies of silicon coated by organic monolayers (alkylsiloxanes). *Phys. Rev. B* **41**, 1111–1128. (doi:10.1103/PhysRevB.41.1111)

Vlachy, V. 1999 Ionic effects beyond Poisson–Boltzmann theory. *Annu. Rev. Phys. Chem.* **50**, 145–165. (doi:10.1146/annurev.physchem.50.1.145)

Westphal, O. & Jann, K. 1965 Bacterial lipopolysaccharides. *Methods Carbohydr. Chem.* **5**, 83.